



## Status of MARS Code\*

Nikolai V. Mokhov<sup>†</sup>

*Fermi National Accelerator Laboratory*

*P.O. Box 500, Batavia, Illinois 60510, USA*

March 24, 2003

### Abstract

Status and recent developments of the MARS14 Monte Carlo code system for simulation of hadronic and electromagnetic cascades in shielding, accelerator and detector components in the energy range from a fraction of an electronvolt up to 100 TeV are described. These include physics models both in strong and electromagnetic interaction sectors, variance reduction techniques, residual dose, geometry, tracking, histogramming, *MAD-MARS Beam Line Builder* and Graphical-User Interface. The code is supported worldwide, see <http://www-ap.fnal.gov/MARS/> and MARS discussion list [mars-forum@fnal.gov](mailto:mars-forum@fnal.gov).

---

\*Presented Paper at the *Shielding Aspects of Accelerators, Targets and Irradiation Facilities (SATIF-6) meeting*, SLAC, Menlo Park, Ca., April 10-12, 2002.

<sup>†</sup>Work supported by the Universities Research Association, Inc., under contract DE-AC02-76CH00300 with the U. S. Department of Energy.

# 1 Introduction

The MARS code system is a set of Monte Carlo programs for detailed simulation of hadronic and electromagnetic cascades in an arbitrary 3-D geometry of shielding, accelerator and detector components with energy ranging from a fraction of an electronvolt up to 100 TeV. The current MARS14 version [1] combines the well established theoretical models for strong, weak and electromagnetic interactions of hadrons and leptons with a system which can contain up to  $10^5$  objects, ranging in dimensions from microns to hundreds of kilometers, made of up to 100 composite materials, with arbitrary 3-D magnetic and electric fields, and a powerful user-friendly Graphical-User Interface for visualization of the geometry, materials, fields, particle trajectories and results of calculations. The code has been developed since 1974 at IHEP, SSCL and Fermilab.

In an inclusive mode, the code is capable of fast cascade simulations even at very high energies. MARS tabulates the particles which pass through various portions of the geometry (that can be very simple to very complex), and produces results on particle fluxes, spectra, energy deposition, material activation, and many other quantities. The results are presented in tables, histograms, and other specialized formats. The system also includes physics of the MCNP code for low-energy neutron transport, and interfaces to ANSYS for thermal and stress analyses, MAD for accelerator and beam-line lattice description, and STRUCT for multi-turn particle tracking in accelerators. Various biasing and other variance reduction techniques are implemented in the code. MARS14 allows the user extensive control over the simulation's physics processes, tabulation criteria, and runtime optimizations, via a wide variety of options and switches implemented from an input file, and via the provided customizable user subroutines.

The code is used in numerous applications worldwide (US, Japan, Europe, Russia) at existing accelerator facilities, in planned experiments and accelerator projects ( $pp$ ,  $e^+e^-$  and  $\mu^+\mu^-$  colliders and detectors, kaon and neutrino fixed target experiments, neutrino factories, spallation neutron sources etc.) and in cosmic ray physics. Its reliability has been demonstrated in many benchmark studies. Physics models, geometry, tracking algorithms, Graphical-User Interface (GUI) and other details of the MARS14 code are described in Ref. [1]. Here we highlight just most recent developments to the current version which further increase the code reliability, applicability and user friendliness.

## 2 Physics Model

**Event Generator.** Hadron and photonuclear interactions at  $1 \text{ MeV} < E_0 < 2 \text{ GeV}$  are done via full exclusive simulation with the latest version of the Cascade-Exciton Model CEM [2]. Inclusive particle production via a set of improved phenomenological models is used as a default for  $hA$  and  $\gamma A$  interactions at  $5 \text{ GeV} < E_0 < 100 \text{ TeV}$ ,  $dA$  at  $20 \text{ MeV} < E_0 < 50 \text{ GeV}$  and  $\nu A$  at  $0.1 \text{ GeV} < E_0 < 100 \text{ TeV}$ . A model which combines both of the above approaches is used at  $2 \text{ GeV} < E_0 < 5 \text{ GeV}$  for smooth transition between high and low energy regions. Fig. 1 shows the calculated pion spectra in comparison with recent BNL data. In exclusive mode, the latest version DPMJET-III of the Dual Parton Model [3] can be used for full event generation of a first nuclear collision  $hA$ ,  $AA$ ,  $\gamma A$  and  $\nu A$  at  $E_0 > 5 \text{ GeV}$ . In the same way, the

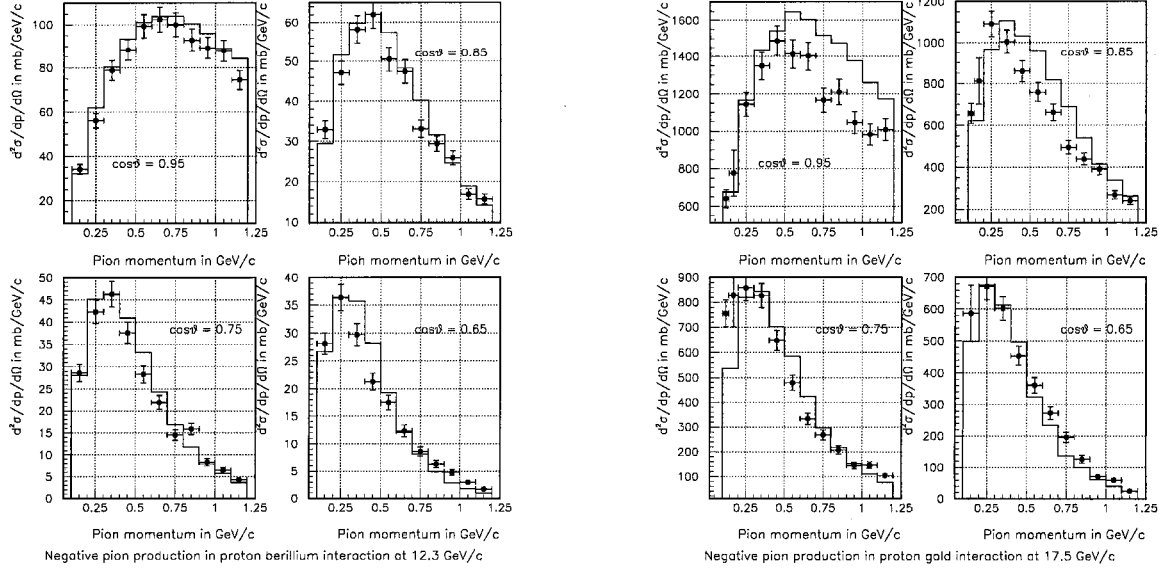


Figure 1:  $\pi^-$  spectra in  $pBe$  at 12.3 GeV/c (left) and in  $pAu$  at 17.5 GeV/c (right) as calculated with MARS14 (histogram) and measured in the BNL E-910 (symbols).

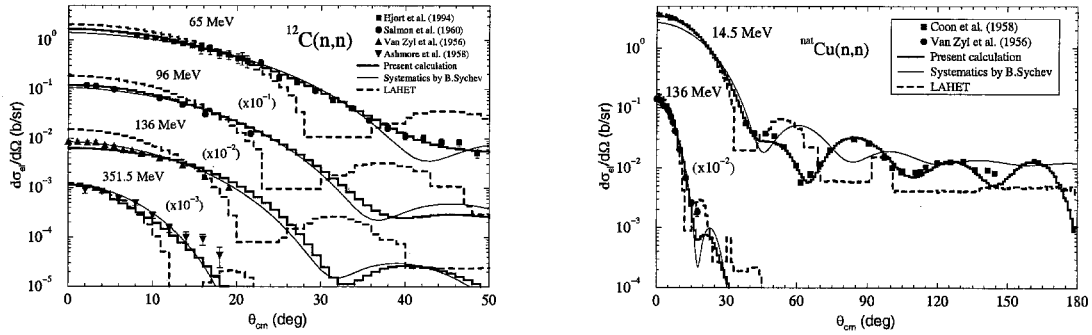


Figure 2: Calculated and measured neutron elastic scattering distributions on carbon (left) and copper (right) nuclei.

LAQGSM code based on the Quark-Gluon String Model [4] has been recently implemented into MARS at  $E_0 < 100$  GeV and successfully used for the first time as described in Ref. [5]. Nuclide production simulation has been added to the code. Antiproton annihilation algorithms have been substantially improved in MARS14.

**Elastic Scattering.** The MARS14 elastic model at  $E < 5$  GeV is based on evaluated nuclear data from the LA-150 and ENDF/HE-VI libraries [6] and Ref. [7, 8] supplied with phenomenology where needed [9]. For protons, nuclear and Coulomb elastic scattering as well as their interference are taken into account. At  $E > 5$  GeV, a simple analytical description used in the code for both coherent and incoherent components of  $d\sigma/dt$  is quite consistent with experiment.

**Interface to MCNP.** Once the energy of neutrons falls below 14 MeV, all subsequent neutron interactions are described using the appropriate MCNP4C2 [10] subroutine modules. Secondaries generated at this stage by neutrons – protons, photons and deuterons –

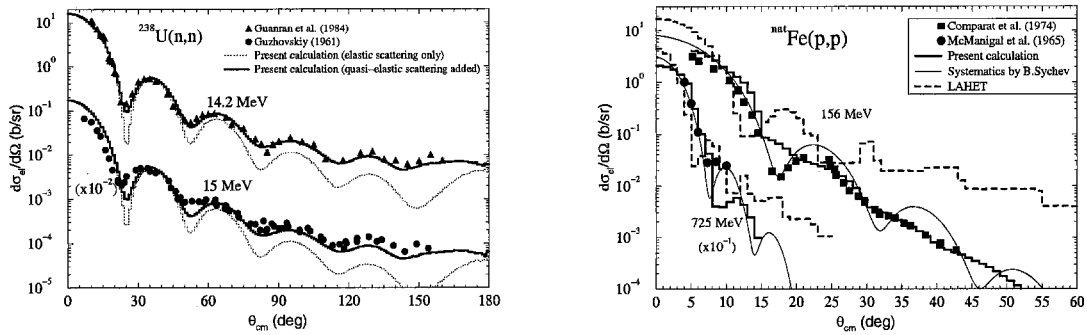


Figure 3: Calculated and measured elastic scattering distributions for neutrons on uranium (left) and protons on iron (right).

are directed back to the MARS modules for a corresponding treatment. This implementation, along with algorithms developed for heavier recoils and photons from the thermal neutron capture on  ${}^6\text{Li}$  and  ${}^{10}\text{B}$ , allows the detailed description of corresponding effects in hydrogenous, borated and lithium-loaded materials. The interface includes several other modifications to the dynamically allocated storage, material handling, optional writing of low-energy neutrons and other particles to a file for further treatment by a standalone MCNP code and MCNP geometry description (see below).

**Coulomb Scattering.** Since 1985 multiple Coulomb scattering was modeled in MARS from the Moliere distribution with the Gaussian nuclear form-factor included. Just recently, a new algorithm was developed and implemented into MARS14. It provides about a per cent accuracy for stepsizes ranging from a few collisions to thousands of radiation lengths in arbitrary mixtures, taking into account nuclear screening with an arbitrary form-factor. The algorithm is based on splitting scattering into “soft” and “hard” parts with a cutoff angle  $\theta_{max}$  calculated automatically depending on the stepsize and other input parameters. A “soft” small-angle distribution is sampled from a near-Gaussian asymptotic, while “hard” discrete collisions ( $0 \leq N_{disc} \leq 20, \langle N_{disc} \rangle \sim 1$ ) are sampled from a single scattering differential cross-section.

### 3 Variance Reduction

Many processes in MARS14, such as electromagnetic showers, most of the hadron-nucleus interactions, decays of unstable particles, emission of synchrotron photons, photohadron production and muon pair production, can be treated either analogously or inclusively with corresponding statistical weights. The choice of method is left for the user to decide, via the input settings. Other variance reduction techniques are used in the code: weight-window, splitting and Russian roulette, exponential transformation, probability scoring, step/energy cutoffs. Depending on a problem, these techniques are thoroughly utilized in the code to maximize computing efficiency, which is proportional to  $t_0/t$ . Here  $t$  is CPU time needed to get a RMS error  $\sigma$  equal to the one in the reference method with CPU time  $t_0$ , provided  $\sigma \leq 20\text{-}30\%$ . An example of one history for a 1-GeV positron on a 2-cm tungsten target

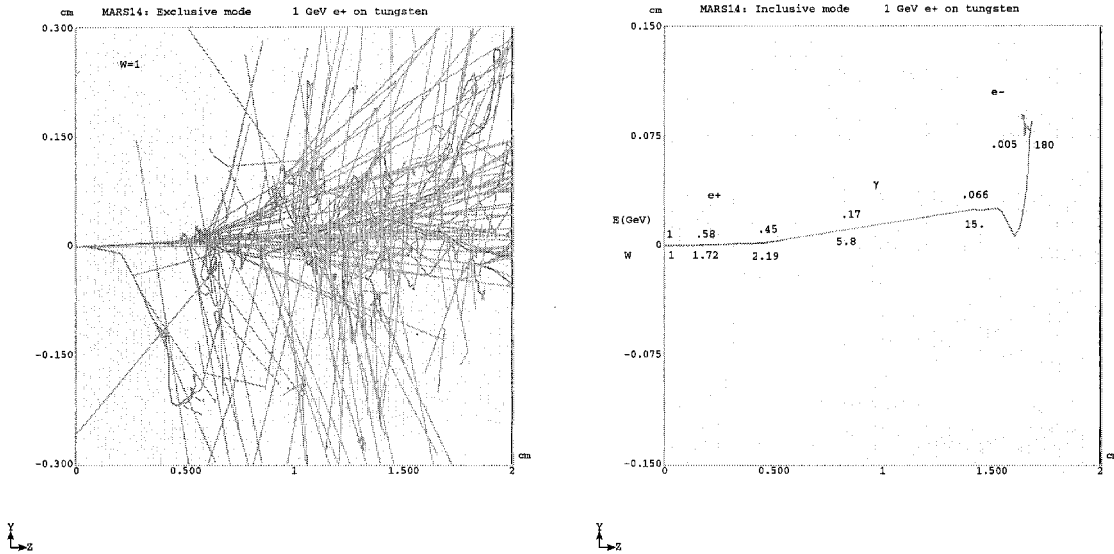


Figure 4: 1-GeV positron on 2-cm tungsten target: one history simulated in exclusive mode (left) and Leading Particle Biasing mode (right).

calculated in MARS14 in exclusive and leading particle biasing modes is given in Fig. 4. It was found empirically that the biasing scheme for  $hA$  vertex shown in Fig. 5 and used in the code for years, provides the highest efficiency  $\epsilon$  in detector, accelerator and shielding applications. Here a fixed number and types of secondaries are generated with the appropriate statistical weights.

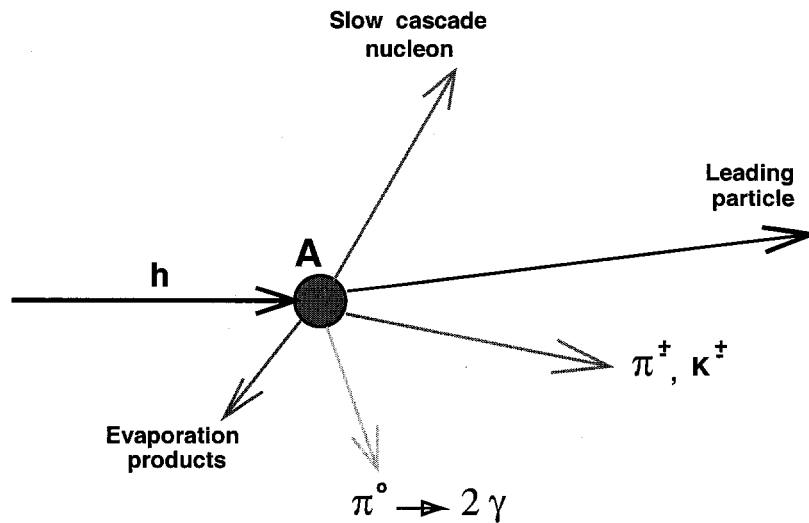


Figure 5: MARS inclusive nuclear interaction vertex.

## 4 Residual Dose

A substantially improved  $\omega$ -factor based algorithm [11] to calculate residual dose rates in arbitrary composite materials for arbitrary irradiation and cooling times was developed and implemented into the code. The algorithm distinguishes three major energy groups responsible for radionuclide production: (1) above 20 MeV, (2) 1 to 20 MeV, and (3) below 0.5 eV. The energy groups are chosen to consider separately the most important nuclear reactions responsible for induced radioactivation in the regions: high energy inelastic interactions (mostly spallation reactions), threshold reactions ( $n, 2n$ ), ( $n, p$ ) etc, and ( $n, \gamma$ ) reactions, respectively. Neutrons in the energy region from 0.5 eV to 1 MeV do not produce a significant number of radionuclides. Creation of the residual nuclides was pre-calculated with a version [12] of the FLUKA code for cascades induced by energetic hadrons in cylindrical samples of 17 elements: C, O, Na, Mg, Al, Si, K, Ca, Cr, Fe, Ni, Cu, Nb, Ag, Ba, W, Pb. The decay chains of the created radionuclides were followed with the DETRA code in order to determine the emission rates of de-excitation photons for irradiation time  $12 \text{ hours} < T_i < 20 \text{ years}$  and cooling time  $1 \text{ sec} < T_c < 20 \text{ years}$ . Corresponding dose rates on the outer surfaces were calculated from photon fluxes and related to the star density above 20 MeV (first group), and neutron fluxes in two other energy groups. Results were collected in a database, that – along with a sophisticated interpolation algorithm linked to this database – was implemented into MARS14. An example of residual dose calculation for a pump and cryostat of the Fermilab MUCOOL experiment for a 400-MeV proton beam at  $1.5 \times 10^{14} \text{ p/s}$  is shown in Fig. 6.

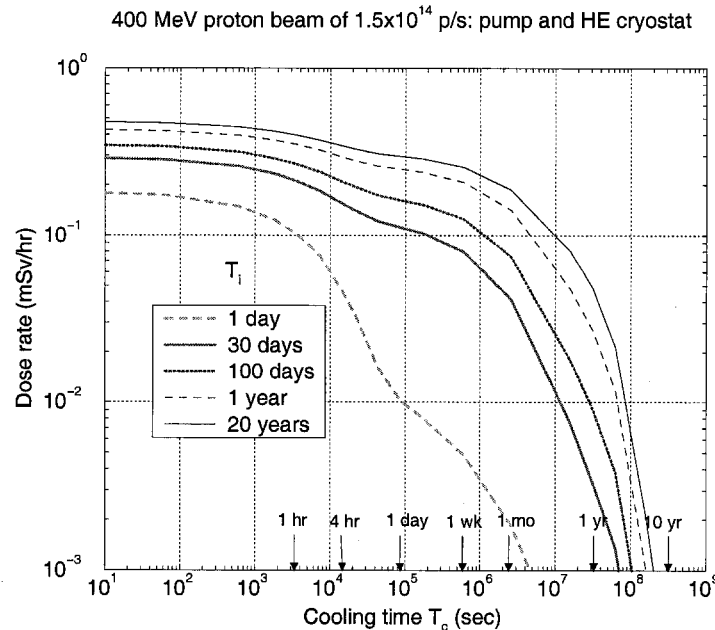


Figure 6: Example of MARS14 residual dose calculation in the Fermilab MUCOOL experiment.

## 5 Geometry

Volumes of *non-standard* regions in MARS14 can now be calculated in a short Monte Carlo session. A corresponding output file provides calculated volumes with statistical errors, global and non-standard region numbers, and is directly linked to the main code.

In addition to widely used *Standard* and *Non-standard* geometries in MARS14, a drastically improved *Extended Geometry* option is now available in the code. *Extended* zones are constructed from a set of contiguous or overlapping geometrical shapes, currently, boxes, spheres, cylinders, and truncated cones and tetrahedrons. A variety of new features, such as up to 100000 extended volumes, subdivision of volumes into subregions, up to 500 arbitrary transformation matrices etc, are there. There is no worry now about missing a small object in a large mother volume. Fig. 7 shows an example of an extended geometry setup with particle tracks induced by a 50-GeV proton.

A new fourth geometry option is now available in MARS14, the *MCNP* one. A MCNP geometry description can now be put in the MCNP section of the MARS.INP input file and used directly by the MARS14 code. The MCNP community interested in high-energy applications, can now use MARS14 with their MCNP geometry packages.

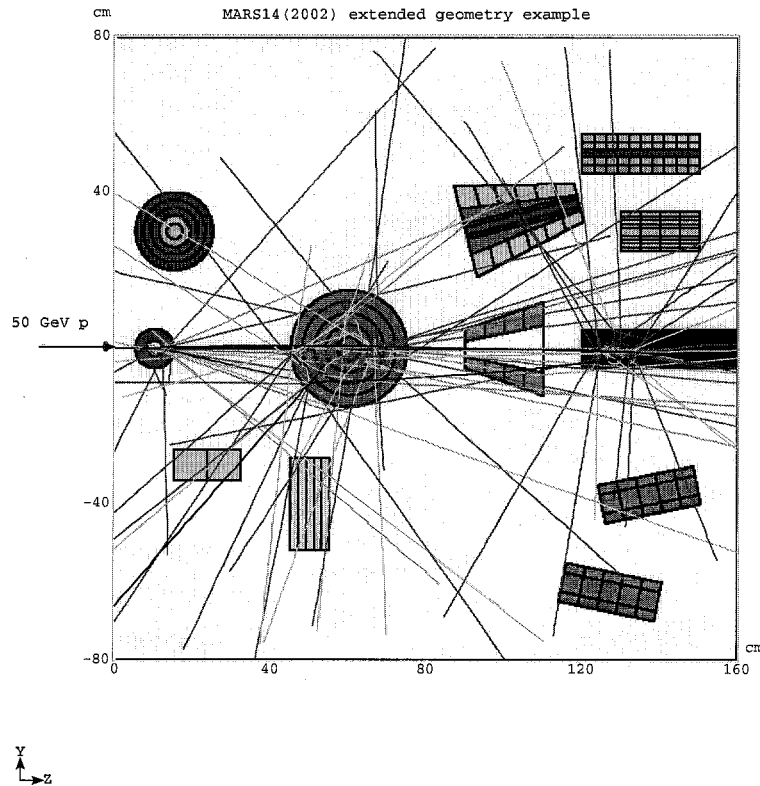


Figure 7: An example of MARS14 extended geometry with particle tracks.

## 6 Materials, Tracking and Histograming

There are 135 built-in materials in MARS14 plus arbitrary user-defined compounds. A maximum of 100 materials can be used within any simulation. A material can be declared multiple times in the input file, so that different step-size or energy thresholds can be applied to the same material. This feature allows noticeable improvement of both a CPU performance and physics description accuracy in the regions of interest. The precise treatment of individual elements in mixtures and compounds defined through the weight or atomic fractions, is done for all the electromagnetic and nuclear elastic and inelastic processes. The appropriate parameters for particle transport in arbitrary magnetic fields are chosen automatically, providing extremely high accuracy of tracking. The phase-space/geometry tagging module was further improved. A *Global Shielding parameter set* was added to the code allowing substantial CPU time savings for “a deep penetration” problem and other cases with thick extended shieldings. A variety of built-in and user-defined histograming was further extended. Recently, a possibility for histograming with a histogram origin that follows the curvature of beam lines and accelerator arcs (see next section) was added to MARS14.

## 7 MAD-MARS Beam Line Builder

A further developed interface system—*MAD-MARS Beam Line Builder* (MMBLB)—reads a MAD lattice file and puts the elements in the same order into MARS geometry. Each element is assigned six functions which provide information about the element type/name, geometry, materials, field, volume and initialization. The user specifies the element type and an optional element name. A building algorithm first tries to match the type/name pair and then substitute a generic element if needed. Once an element is described, it is registered with the system and its name is bound with the respective geometry, materials, volume and field descriptions. For each region search during tracking, MMBLB finds the corresponding type/name pair and calls its appropriate functions. MMBLB calculates a local rotation matrix  $\mathcal{R}_i$  and a local translation vector  $\mathcal{L}_i$ . Then a global rotation matrix  $\mathcal{M}_i$  and a position  $\mathcal{P}_i$  are calculated and stored for each element.

## 8 Graphical-User Interface

The Graphical-User Interface, MARS-GUI-SLICE was further developed. It is based on *Tcl/Tk* and is linked in to the user’s executable. The interface displays all the details of the encoded geometry, showing the encoded zone numbers, materials and magnetic fields; it is a valuable tool for checking complex geometries before executing event generation. Arbitrary 3-D rotation of a slice is possible. During event generation runs, the user can specify output files holding histograms and particle tracks; these output files can be opened by the *GUI* interface, post-run, and projected onto the visual display of the geometry.

A new three-dimensional visualization engine has been recently developed [13] for the MARS14 code. It further extends the power of visualization adding a crucial in many

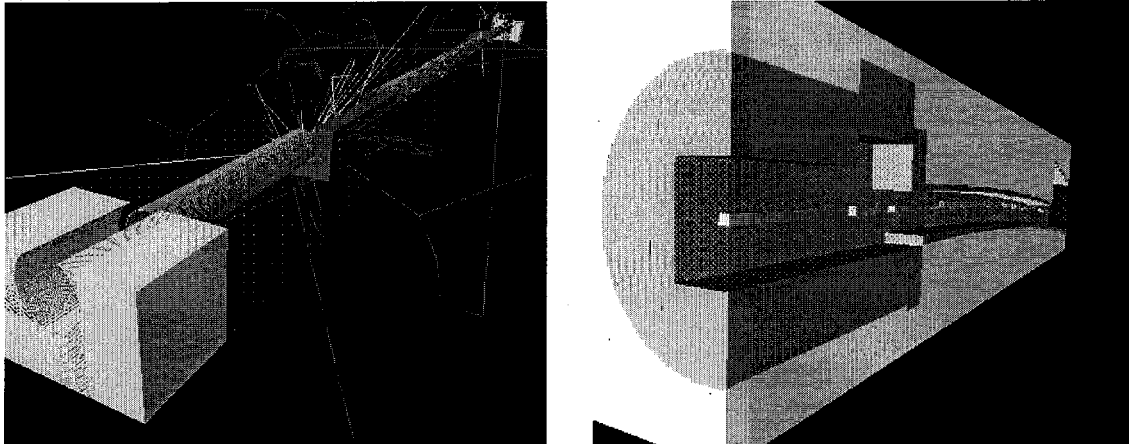


Figure 8: Details of the Fermilab Booster collimation section with “L” shaped collimators and particle tracks (left) and a fragment of the NuMI beamline and tunnel (right).

instances three-dimensional view of the system studied. It is based on the OPENINVENTOR graphics library, integrated with MARS-GUI-SLICE and uses a sophisticated optimization algorithm developed for arbitrary *non-standard* geometry in MARS. Fig. 8 presents two recent examples at Fermilab Booster and NuMI created with this new powerful tool.

## 9 Acknowledgments

Thanks to K. Gudima, M. Huhtinen, C. James, M. Kostin, O. Krivosheev, S. Mashnik, I. Rakhno, J. Ranft, S. Roesler, J. Rzepecki, S. Striganov, I. Tropin, A. Wehmann for collaboration and useful discussions.

## References

- [1] N.V. Mokhov, “The MARS Code System User’s Guide”, Fermilab-FN-628 (1995); N.V. Mokhov, O.E. Krivosheev, “MARS Code Status”, *Proc. Monte Carlo 2000 Conf.*, p. 943, Lisbon, October 23-26, 2000; Fermilab-Conf-00/181 (2000); <http://www-ap.fnal.gov/MARS/>.
- [2] S.G. Mashnik, A.J. Sierk, “CEM2k—Recent Developments in CEM”, *Proc. AccApp00 (Washington DC, USA)*, pp. 328–341, La Grange Park, IL, USA, 2001 (nucl-th/001116); S.G. Mashnik, A.J. Sierk, “Recent Developments of the Cascade-Exciton Model of Nuclear Reactions”, *Proc. ND2001 (Tsukuba, Japan)*, *J. Nucl. Sci. Techn.*, Supplement 2, 720–725, 2002; Eprint: [nucl-th/0208074](http://arxiv.org/abs/nucl-th/0208074).
- [3] J. Ranft, “Dual Parton Model at Cosmic Ray Energies”, *Phys. Rev.* **D51**, 64–85 (1995); Gran Sasso Report INFN/AE-97/45 (1997); S. Roesler, R. Engel, J. Ranft, “The Monte Carlo Event Generator DPMJET-III”, *Proc. Monte Carlo 2000 Conf.*, p. 1033, Lisbon, October 23-26, 2000; S. Roesler, R. Engel, J. Ranft, “The Event

- Generator DPMJET-III at Cosmic Ray Energies”, *Proc. ICRC-2011 Conference*, 439, Copernicus Gesellschaft (2001).
- [4] K.K. Gudima, S.G. Mashnik, A.J. Sierk, “User Manual for the Code LAQGSM”, Los Alamos National Report LA-UR-01-6804 (2001).
- [5] J.D. Cossairt, N.V. Mokhov, “Assessment of the Prompt Radiation Hazards of Trapped Antiprotons”, Fermilab-Pub-02/043-E-REV (2002).
- [6] M.B. Chadwick, P.G. Young, S. Chiba et al., “Cross-Section Evaluations to 150 MeV for Accelerator-Driven Systems and Implementation in MCNPX”, *Nucl. Sci. Eng.*, **131**, 293 (1999).
- [7] S. Chiba, O. Iwamoto, E.Sh. Sukhovitski et al., “Coupled-Channels Optical Potential for Interaction of Nucleons with  $^{12}\text{C}$  up to 150 MeV in Soft-Rotator Model”, *J. of Nuclear Science and Technology*, **37**, 498 (2000).
- [8] E.Sh. Sukhovitski, Y.-O. Lee, J. Chang et al., “Nucleon Interaction with  $^{58}\text{Ni}$  up to 150 MeV studied in the coupled-channels approach based on the soft-rotator nuclear structure model”, *Phys. Rev. C*, **62**, 044605-1 (2000).
- [9] I.L. Rakhno, N.V. Mokhov, E. Sukhovitski, S. Chiba, “Simulation of Nucleon Elastic Scattering in the MARS14 Code System”, *Proc. of the ANS Topical Meeting on Accelerator Applications/Accelerator Driven Transmutation Technology Applications, AccApp/ADTTA’01*, Reno, Nevada, Nov. 11-15, 2001, Ominpress CD ROM (2002), ISBN: 0-89448-666-7; Fermilab-Conf-01/343-T (2001).
- [10] J.F. Briesmeister, editor: “MCNP – A General Monte Carlo N-Particle Transport Code”, Version 4A, Pub. LA-12625-M, LANL (1993).
- [11] I.L. Rakhno, N.V. Mokhov, A. Elwyn, N. Grossman, M. Huhtinen, L. Nicolas, “Benchmarking Residual Dose Rates in a NuMI-like Environment”, in Ref. [9]; Fermilab-Conf-01/304-E (2001).
- [12] P. Aarnio, *et al.*, CERN/TIS-RP/93-10; A. Fassò, *et al.*, *Proc. IV Int. Conf. on Calorimetry in High Energy Physics*, La Biodola, Sept 20-25, 1993, Ed. A. Menzione and A. Scribano, World Scientific, p. 493 (1993); A. Fassò, *et al.*, *Proc. Specialists’ Meeting on Shielding Aspects of Accelerators, Targets and Irradiation Facilities*, Arlington, Texas, April 28-29, 1994. NEA/OECD doc., p. 287 (1995).
- [13] J.P. Rzepecki, M.A. Kostin, N.V. Mokhov, “3D Visualization for the MARS14 Code”, Fermilab-TM-2197 (2003).